FINITE-PRECISION DESIGN AND IMPLEMENTATION OF ALL-PASS POLYPHASE NETWORKS FOR ECHO CANCELLATION IN SUB-BANDS

O. Tanrikulu, B. Baykal, A. G. Constantinides, J. A. Chambers and P. A. Naylor

Department of Electrical and Electronic Engineering,
Imperial College of Science, Technology and Medicine, London SW7 2BT, UK.

ABSTRACT

All-pass Polyphase Networks (APN) are particularly attractive for Acoustical Echo Cancellation (AEC) arranged in sub-bands. They provide lower inter-band aliasing, delay and computational complexity than their FIR counterparts. Moreover, APNs achieve higher Echo Return Loss Enhancement (ERLE) performance and faster convergence than full-band processing. In this paper, the finite precision implementation of APNs is addressed. A procedure is presented for re-optimising the all-pass coefficients of the prototype low-pass filter for finite precision operation. Robust finite precision implementation of a prototype low-pass filter is discussed. The results of a set of AEC experiments are reported with full and 16-bit precision implementation.

I. INTRODUCTION

In AEC, traditional approaches use either centre clipping or adaptive synthesis and subtraction of the echo signal. The latter is an elegant solution to the problem but the computational constraints imposed by real-time operation, and the length of the acoustic path impulse response, often make it unviable to use simple adaptive algorithms such as Normalised Least Mean-Square (NLMS).

Signal Processing in sub-bands offers many advantages [1]. The main processing is carried out at a lower rate which reduces the computational complexity. Other benefits are faster convergence and lower residual echo power as compared to full-band processing with NLMS.

Sub-band division using FIR filters can be implemented efficiently as polyphase networks as in Figure 1 where $H_i(z^{-M})$ are the FIR polyphase components of the prototype low-pass filter $H(z^{-1})$ [2]. $H(z^{-1})$ has an undecimated lower stop-band cut-off frequency of $\omega_s = (\pi/M)+\varepsilon$, $\varepsilon > 0$. In addition, $H(z^{-1})$ and $H_i(z^{-M})$ are related by,

$$H(z^{-1}) = \sum_{i=0}^{M-1} z^{-i} H_i(z^{-M}). \qquad (1)$$

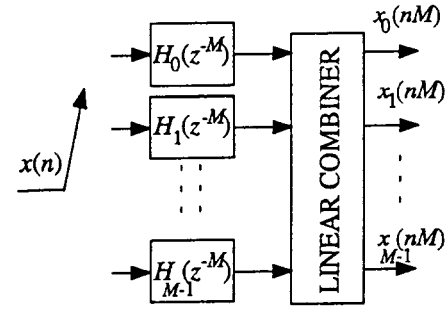

Figure 1 Polyphase M-band division

Perfect reconstruction FIR filter banks provide an alias free signal by combining the outputs of the analysis block with an appropriately designed synthesis block [1,2]. However, a significant point to observe is that while perfect reconstruction is realised, the spectral contents of $x_i(nM)$, i=0,...,M-1 are not entirely disjoint due to the non-ideal nature of the analysis filters. Thus, the insertion of adaptive filters within each sub-band will disturb the perfect reconstruction condition and may thereby introduce high levels of inter-band aliasing within the re-synthesised, full-band, signal. IIR sub-band division filters with sharp transition-band and high stop-band attenuation appear therefore to be very attractive candidate filters for use within an AEC structure.

II. IIR FILTER DESIGN USING ALL-PASS NETWORKS

In [4,5], IIR filter design with all-pass networks is set out in detail. Such a filter is defined by substituting

$$H_i(z^{-1}) = \prod_{j=0}^{P_i-1} \frac{\alpha_{i,j} + z^{-1}}{1+\alpha_{i,j} z^{-1}}, \qquad (2)$$

in (1) where P_i is the number of all-pass coefficients at the i^{th}-phase. The all-pass coefficients $\alpha_{i,j}$ can be obtained by using nonlinear optimisation techniques that minimise the stop-band power. The amplitude response and the pole-zero diagram of a typical all-pass prototype with $P_0 = 6$, $P_1 = 5$ and ω_s = 1.608 rad. is shown in Figure 2. The

0-7803-2431-5/95 $4.00

stop-band attenuation is approximately 100dB and the transition band is very narrow.

APNs are the polyphase configuration of the prototype IIR filter defined by (1) and (2) as shown in Figure 1. APNs provide perfect amplitude reconstruction but the phase reconstruction is non-ideal due to the non-linear phase response of the all-pass sections. However, this is not important in AEC since the phase distortion introduced by APNs is normally not discerned by the human auditory system [7].

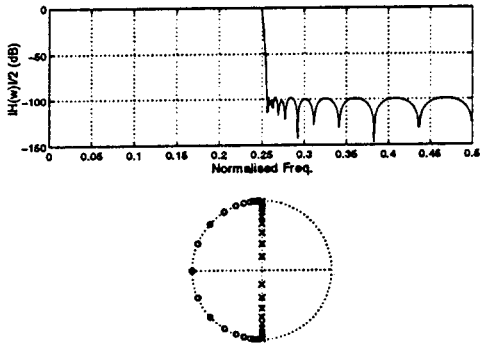

Figure 2 $|H(\omega)|$, pole-zero plot with full precision all-pass coefficients.

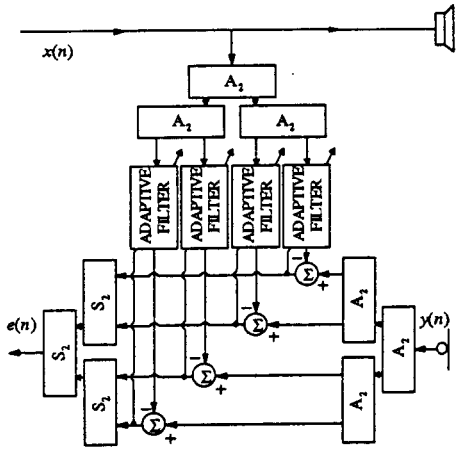

Figure 3 Four-band AEC Structure

III. AEC STRUCTURE

Uncontrolled peaks occur in the amplitude spectrum of the IIR low-pass prototype at $\omega_i = i\pi/M$, $\{M>2,\ i>1\}$ when $\omega_s = (\pi/M)+\varepsilon$, $\varepsilon > 0$ [4]. Therefore, the most appropriate sub-band decomposition based upon APNs is two-band. This case can serve as a building block for higher order decompositions ($M > 2$) and a binary tree structure can be used. The AEC structure for $M = 4$, is shown in Figure 3 where A_2 and S_2 denote respectively the two-band polyphase analysis and synthesis blocks. Note that, in the specific application we direct our attention, $x(n)$ is the far-end speech and $y(n)$ is the microphone signal at the near-end which contains the acoustical echo.

IV. RE-OPTIMISATION OF ALL-PASS COEFFICIENTS

Although all-pass networks are robust to finite precision effects [4,6], an undesirable degree of degradation may occur for sharp low-pass prototypes with very high stop-band attenuation. This is due to the slight mismatch in the all-pass phase responses. Thus, in a finite precision filter realisation instead of rounding the all-pass coefficients to the nearest integer value after scaling, they can be re-optimised by using the full precision all-pass coefficients as a starting point and then solving the problem,

$$\min_{\alpha_{i,j}\in(0,2^{b-1}-1]}\left\{\max_{\omega\in[\omega_s,\pi]}\left\|H(\omega)\right|-\left|H_f(\omega)\right\|\right\} \qquad (3)$$

where b is the number of bits representing the available precision, while $H(\omega)$ and $H_f(\omega)$ are the spectra obtained by using full-precision and finite-precision all-pass coefficients respectively. A suboptimal solution of (3) can be obtained as follows:

1. Scale $\alpha_{i,j}$ such that the interval [0,1] is mapped onto $[0,2^{b-1}-1]$.
2. Choose the maximum all-pass coefficient.
3. Round the chosen all-pass coefficient to the next lower or higher integer which ever yields a smaller distance to the stop-band characteristics of $H(\omega)$.
4. Keep the rounded all-pass coefficients as constant and vary the others to solve (3).
5. Obtain the next smaller all-pass coefficient and goto 3 until the above procedure is carried out for all all-pass coefficients.

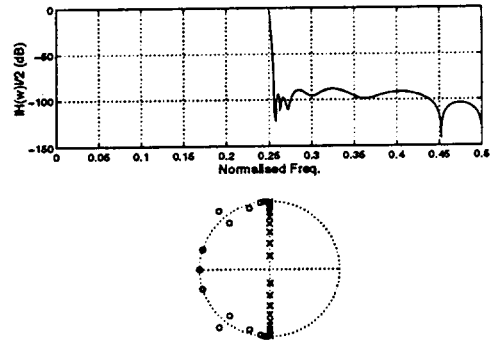

Figure 4 $|H(\omega)|$, pole-zero plot via 16-bits rounding

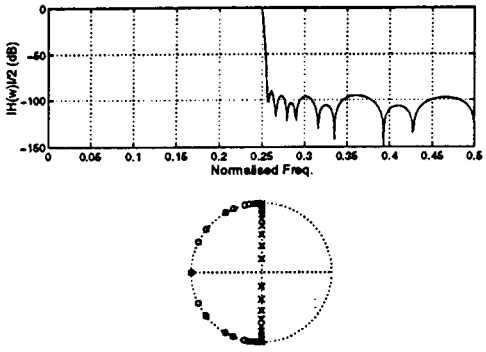

Figure 5 $|H(\omega)|$, pole-zero plot via re-optimisation

The filter characteristics obtained by rounding and re-optimisation are shown respectively in Figure 4 and Figure 5. It is evident that the optimisation yields characteristics closer to those in Figure 2 by keeping the zeros on the unit circle.

V. FINITE-PRECISION IMPLEMENTATION OF AEC

In the prototype IIR low-pass filter, the all-pass section with the maximum all-pass coefficient is most sensitive to the multiplication round-off noise. Therefore, in the 16-bit implementation of the prototype low-pass filter in Figure 2, all-pass sections should be cascaded such that the magnitude of the coefficients is increasing. This yields improved stop-band characteristics. The signal flow graph used in the implementation of first order all-pass sections has a profound effect on the filter characteristics. In [6], four compact (single multiplier) realisations of a first order all-pass function are considered and the output noise due to multiplication round-off is given as function of all-pass coefficient value. Since the poles of the prototype IIR low-pass filter are on the imaginary axis, the particular signal flow graphs shown in Figure 6 are used depending upon the value of the all-pass coefficients.

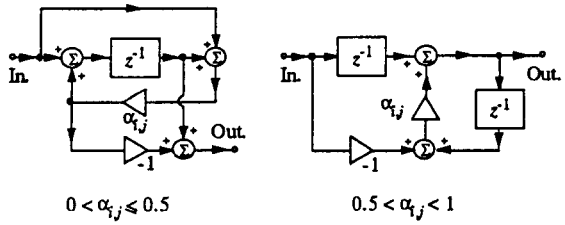

Figure 6 Compact first-order all-pass realisations.

The amplitude characteristics given by the canonical (*i.e.* two multiplier, one delay) and compact implementations of the prototype IIR low-pass filter are shown in Figure 7. It is observed that for the canonical implementation there is significant degradation at the transition-band and stop-band characteristics. Moreover, there is a limit cycle at $\theta = 0.25$. When the compact realisations in Figure 6 are employed, it is clear that the stop-band characteristics are improved drastically and the limit cycle disappears.

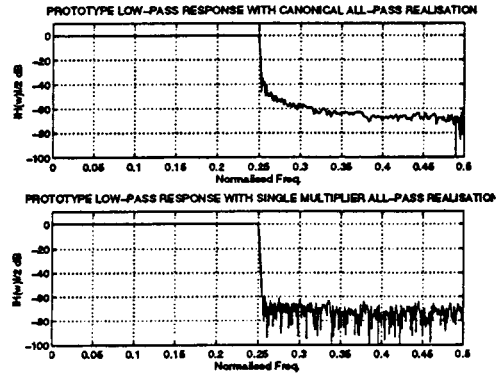

Figure 7 16-bit prototype filter realisations

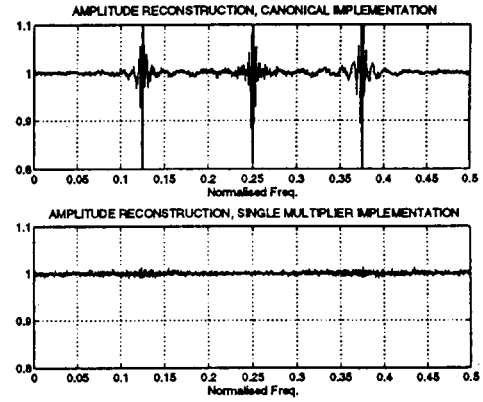

Figure 8 Amplitude reconstruction in 16-bit precision.

The analysis and synthesis blocks in APN achieve perfect amplitude reconstruction in infinite precision [3]. However, the quality of amplitude reconstruction in finite precision is degraded significantly if the canonical implementation is used instead of the chosen implementations. This is illustrated in Figure 8 for cascaded four-band analysis and synthesis blocks.

VI. SIMULATIONS

AEC experiments are carried out in an office environment in order to demonstrate the effect of finite precision implementation of the analysis and synthesis blocks. Male (FC, JB) and female (MH, SM) speakers were asked to utter the French sentence, "Paris Bordeaux Le Mans Saint-Leu Léon Loudun" which is sampled at 8 KHz. AEC is performed in the single-talk situation when there is no ambient noise. Full-band, full-precision NLMS is applied with 512 adaptive coefficients. The mean and maximum

values of ERLE are computed over 32 msec. of non-overlapping windows. The Time of Initial Convergence (TIC) to 10dB is also obtained. The results are presented in Table 1.

Speaker	max ERLE	mean ERLE	TIC 10dB
FC	15.42 dB	9.37 dB	96 msec.
JB	14.96 dB	7.01 dB	384 msec.
MH	17.43 dB	8.11 dB	416 msec.
SM	20.93 dB	10.01 dB	320 msec.

Table 1 AEC results for full-band, full-precision NLMS.

The four-band AEC structure Figure 3 is used with full-precision and 128 adaptive coefficients are employed in each sub-band. The results are presented in Table 2.

Speaker	max ERLE	mean ERLE	TIC 10dB
FC	20.87 dB	11.83 dB	96 msec.
JB	17.66 dB	10.66 dB	32 msec.
MH	18.79 dB	10.82 dB	96 msec.
SM	22.60 dB	13.38 dB	32 msec.

Table 2 AEC results for full-precision, four-band structure.

Finally, sub-band analysis and synthesis blocks are implemented in 16-bit precision while NLMS still uses full precision and 128 adaptive coefficients in each sub-band. The results are shown in Table 3.

Speaker	max ERLE	mean ERLE	TIC 10dB
FC	20.14 dB	10.88 dB	96 msec.
JB	17.78 dB	10.54 dB	32 msec.
MH	18.60 dB	10.61 dB	96 msec.
SM	22.45 dB	12.72 dB	32 msec.

Table 3 AEC results for 16-bits precision sub-band analysis and synthesis blocks and full-precision NLMS.

The results above demonstrate that using sub-band processing in this area is more advantageous than full-band processing. There is a clear improvement in the ERLE performance and TIC is significantly lower for the results in Table 2 and Table 3. Furthermore, the degradation introduced by the finite precision implementation of the analysis and synthesis blocks in the realisations employed is insubstantial.

VII. CONCLUSIONS

Finite precision implementation of the analysis and synthesis blocks in APNs is addressed in the context of sub-band AEC. The discretisation of the all-pass coefficients is investigated and a scheme is proposed in order to minimise the change in the characteristics of the prototype IIR low-pass filter for finite-precision operation. Compact first-order realisations of the all-pass sections is utilised and multiplication round-off noise is minimised. The quality of amplitude reconstruction is compared for canonical and compact realisations of the first-order all-pass sections. A set of AEC experiments is carried out in an office environment under a single-talk situation with no ambient noise. The results clearly demonstrate the advantage of using APNs and their robustness in finite-precision implementation. AEC with APNs are more favourable than full-band and classical FIR sub-band processing in terms of performance, computational complexity and delay.

ACKNOWLEDGEMENTS

This work is funded by EC project no. 6166, "FREETEL". Databases are provided by the FREETEL consortium. Authors would like to thank Matra Communications, ENST, PAGE Iberica, LTSI and ILSP.

REFERENCES

[1] A. Gilloire and M. Vetterli, "Adaptive filtering in sub-bands with critical sampling: analysis, experiments and application to acoustic echo cancellation," *IEEE. Trans. Sig. Proc.*, vol.40, pp. 320-328, April 1994.

[2] P. P. Vaidyanathan, *Multirate Systems and Filter Banks*, New Jersey, Prentice-Hall, 1993.

[3] J. E. Hart, P. A. Naylor and O. Tanrikulu, "Polyphase Allpass IIR Structures for Sub-band Acoustic Echo Cancellation," *EUROSPEECH-93*, Berlin, vol. 3, pp. 1813-1816, Sept. 1993.

[4] R.A. Valenzuela and A. G. Constantinides, "Digital Signal Processing schemes for efficient interpolation and decimation," *IEE Proc.*, vol. 130, no. 6, pp. 225-235, Dec. 1983.

[5] F. Harris, M. O. Lantremange and A. G. Constantinides, "Digital Signal Processing with Efficient Polyphase Recursive All-pass Filters," *Int. Conf. Sig. Proc.*, Florence, Italy, Sept. 1991.

[6] S. K. Mitra and K. Hirano, "Digital All-Pass Networks," *IEEE Trans. Circuits and Systems*, vol. CAS-21, no. 5, pp. 688-700, Sept. 1974.

[7] L. R. Rabiner and R. W. Schafer, *Digital Processing of Speech Signals*, Prentice-Hall, Englewood Cliffs, New Jersey, 1978.